Journal of Chromatography A, 1232 (2012) 65–76

Contents lists available at SciVerse ScienceDirect

Journal of Chromatography A

journal homepage: www.elsevier.com/locate/chroma

Comparison of the quantitative performance of constant pressure versus constant flow rate gradient elution separations using concentration-sensitive detectors

M. Verstraeten[a], K. Broeckhoven[a], F. Lynen[b], K. Choikhet[c], M. Dittmann[c], K. Witt[c], P. Sandra[b,d], G. Desmet[a,*]

[a] Vrije Universiteit Brussel, Department of Chemical Engineering (CHIS-IR), Pleinlaan 2, 1050 Brussels, Belgium
[b] Ghent University, Department of Organic Chemistry, Laboratory of Separation Sciences, Krijgslaan 281 S4-bis, 9000 Gent, Belgium
[c] Agilent Technologies Germany GmbH, Hewlett-Packard Str. 8, BW 76337, Waldbronn, Germany
[d] Research Institute for Chromatography (R.I.C.), President Kennedypark 26, 8500 Kortrijk, Belgium

ARTICLE INFO

Article history:
Available online 12 October 2011

Keywords:
Constant pressure
Peak area
Retention time
Calibration
Viscous heating
Ultra-high pressure

ABSTRACT

This contribution discusses the difference in chromatographic performance when switching from the customary employed constant flow rate gradient elution mode to the recently re-introduced constant pressure gradient elution mode. In this mode, the inlet pressure is maintained at a set value even when the mobile phase viscosity becomes lower than the maximum mobile phase viscosity encountered during the gradient program. This leads to a higher average flow rate compared to the constant flow rate mode and results in a shorter analysis time. When both modes carry out the same mobile phase gradient program in volumetric units, normally identical selectivities are obtained. However, small deviations in selectivity are found due to the differences in pressure and viscous heating effects. These selectivity differences are of the same type as those observed when switching from HPLC to UHPLC and are inevitable when speeding up the analysis by applying a higher pressure. It was also found that, when using concentration-sensitive detectors, the constant pressure elution mode leads to identical peak areas as the constant flow rate mode. Also the linearity is maintained. In addition, the repeatability of the peak area and retention time remains the same when switching between both elution modes.

1. Introduction

All current developments in LC aim at faster and better separations. The latest trends include the application of smaller particles and consequently higher pressures [1–3], fused-core particles [4,5] and high temperatures [6–9]. Recently, the constant pressure mode was introduced as an alternative way to speed up the analysis of gradient LC separations without sacrificing any (when $F \approx F_{opt}$) or only some (when $F \gg F_{opt}$) separation resolution [10,11]. The potential benefit of this operating mode arises from the fact that during the mobile phase gradient separation with a constant flow rate (cF-mode), the kinetic advantage of working at the maximum pressure [12–14] is only exploited for a brief instance when the viscosity is maximum and the maximum pressure is reached. On the other hand, when the pump constantly delivers the maximum pressure (cP-mode) during the gradient separation, the pump will deliver a higher flow rate during most of the gradient, the elution of the components is sped up and the analysis time is shortened. Theoretical calculations showed that a time gain of 15–20% may be expected for a linear gradient from 5 to 95 vol% organic modifier, the gain can either be smaller or larger for other gradient programs and experimental conditions. Considering furthermore that also the safety pressure margin is no longer necessary, an additional time gain of about 5–10% can be added to the aforementioned values. Moreover, the cP-mode can also prevent the occurrence of system failures due to pressure perturbations in the cF-mode.

In [10,11] it was also shown that this gain in analysis time can be obtained without having to make any compromise on the selectivity of the separation as the cP-mode will always lead to similar separation selectivities when the same mobile phase gradient program is applied in volumetric coordinates (% organic modifier vs. run volume), at least when neglecting potential pressure effects [15–19] and viscous heating [20–25]. Volumetric coordinates are also useful for the correct quantification of the separation selectivity and separation efficiency, because the time-based chromatogram no longer correctly represents the separation state in the column when the flow rate varies in time, whereas the volume-based chromatogram still does. For this purpose, a volume-based reconstructed time scale t_V was introduced by dividing the pumped volume V by a constant flow rate value F_F, which in the present

* Corresponding author. Tel.: +32 2629 32 51; fax: +32 2629 32 48.
E-mail address: gedesmet@vub.ac.be (G. Desmet).

0021-9673/$ – see front matter © 2011 Elsevier B.V. All rights reserved.
doi:10.1016/j.chroma.2011.10.019

Nomenclature

C_{found}	mean values of the smallest concentration found [ng/μL]
CC_α	decision limit [ng/μL]
CC_β	detection capability [ng/μL]
cF	constant flow rate operation
cP	constant pressure operation
F	mobile phase flow rate [m^3/s]
F_F	flow rate during a cF-mode run [m^3/s]
F_{max}	maximum experimental flow rate [m^3/s]
F_{min}	minimum experimental flow rate [m^3/s]
LOD	limit of detection [ng]
LOQ	limit of quantification [ng]
n_p	peak capacity [/]
P_{max}	maximum experimental pressure drop [Pa]
SD	standard deviation
t	time [s]
t_A	analysis time [s]
t_G	gradient time [s]
t_R	retention time [s]
t_V	volume-based reconstructed time [s]
Δt_R	difference in retention time between cF- and cP-mode in volume-based reconstructed units [s]
V	volume [m^3]

study was always taken equal to the flow rate imposed during the corresponding cF-run and corresponding to the minimal flow rate encountered during the cP-run:

$$t_V = \frac{V}{F_F} \quad (1)$$

Also the peak area obtained with a concentration-sensitive detector such as a UV-absorption cell has to be considered in volumetric coordinates (or equivalently the reconstructed time units) because the peak area is independent of the flow rate in volumetric units, whereas it is not in time units, where the peak area varies inversely proportional with the flow rate. Similar to the cF-mode, the cP-mode can also be expected to retain the same selectivity when the column permeability is reduced, e.g., because of column ageing. In this case, the applicable flow rate will inevitably lower, but it will nevertheless remain possible to obtain the same selectivity and peak area in a chromatogram expressed in volumetric units or in reconstructed time units (t_V-units), because the selectivity and the peak area are exclusively determined by the volume of mobile phase flowing through the column. Regarding the effect of the operating mode on the column lifetime, it is difficult to predict whether the constant high (maximum) pressure to which the columns are exposed in the cP-mode would either be more or less deleterious than the variable pressure to which the columns are exposed in cF-mode. A comprehensive experimental study of the problem would be needed to understand this.

Comparing the separation efficiency between the cP- and cF-mode separation conducted at the maximum pressure, the cP-mode leads to plate height values that are 20–40% smaller in the B-term dominated regime, e.g. when using very long columns to obtain high efficiency separations – and some 5–10% larger in the C-term dominated regime, e.g., when using short columns for very fast separations (valid for peaks that elute at the maximal flow rate; if the flow rate at elution is lower the increase or decrease in performance will also be smaller). The difference in separation efficiency is caused by the fact that both modes inevitably subject the analytes to a different velocity history [10,11].

The present contribution makes a comparison of the similarity and repeatability of the retention times and peak areas in both elution modes for concentration-sensitive detectors (mainly UV-absorption, but the presented findings are expected to be valid for all concentration-sensitive detectors); calibration curves and the limits of detection are also measured in both elution modes. In order to fully investigate the effects of the differences in pressure and temperature (viscous heating) on the selectivity and resolution in both modes, four different samples with different chromatographic conditions were considered (anti-oxidants, red wine, BSA tryptic digest and a steroid sample).

2. Experimental

All experiments were performed on an Agilent Infinity 1290 System (Agilent Technologies, Waldbronn, Germany), equipped with a firmware that allows constant pressure operation. The firmware of the pump keeps track of the run volume (pumped volume) and adjusts the pumped mobile phase composition according to the gradient program in a way that the composition vs. run volume trace is maintained the same, independent of possible flow rate changes/variations. The 1290 pump was configured with the standard Agilent Jet Weaver V35 mixer. The system also consisted of a diode array detector (DAD) with a low dispersion cell (2 μL volume and 3 mm path length), an autosampler and a thermostatted column compartment. The system was operated with Agilent Chemstation software (modified with a prototype patch to enable volume based operation and data processing) and the obtained chromatographic data was transformed using the pumped volume versus time relationship that the pump keeps track of (see Eq. (1)).

Different samples and chromatographic conditions (columns, temperature and mobile phases) were used to investigate the similarity and repeatability of the separations in constant pressure compared to constant flow rate elution. All chemicals were HPLC-grade and all solvents (ACN, MeOH and H_2O) were purchased from BioSolve, Valkenswaard, The Netherlands and were LC/MS-grade. The experimental procedures and conditions are given for each type of sample below.

Anti-oxidant sample: Propyl gallate (PG), Octyl gallate (OG), Lauryl gallate (LG), tert-butyl-hydroquinone (TBHQ), 2- and 3-tert-butyl-4-hydroxyanisole (BHA), 6-hydroxy-2,5,7,8-tetra-methyl-chromane-2-carboxylic acid (TROLOX) and Ascorbil palmitate (AP) were all purchased from Sigma–Aldrich (Bornem, Belgium). The anti-oxidants were dissolved in methanol at a concentration of 1000 μg/mL and diluted to 100, 50, 20, 10, 5, 2, 1, 0.5 and 0.2 μg/mL. Citric acid and L-isoascorbic acid (purchased from Sigma–Aldrich, Bornem, Belgium) were added to methanol at a concentration of 1 mg/mL to increase the stability of AP in MeOH [26].

The anti-oxidants were separated on a 50 mm Zorbax RRHD Eclipse C18 column (50 mm × 2.1 mm, d_p 1.8 μm, obtained from Agilent Technologies, Waldbronn, Germany). The binary mobile phase consisted of (A) water with 0.02% phosphoric acid and (B) 75/25 ACN:MeOH (v/v). The mobile phase gradient was run from 30 to 100 vol% B in 1.8 min, combined with a column regeneration of 0.2 min (30 vol% B), similar to [27]. The flow rate was set to 1.6 mL/min, corresponding to a pressure drop of 1140 bar at the maximum viscosity. The separation was also conducted at low pressure and with the same volumetric gradient program. The column compartment oven temperature was set to 45 °C; the injection volume was 1.0 μL. All anti-oxidants were detected by UV at a wavelength of 280 nm, except for AP which was detected at 255 nm.

Wine sample: Wine (Chateau Fonreaud, Listrac-Médoc, 2006) was purchased from a local store. The wine was diluted (1:1) with water containing 2% acetic acid (Sigma–Aldrich, Bornem, Belgium) and filtered through a 0.45 μm pore filter.

The wine sample was separated on two coupled 100 mm Zorbax RRHD Eclipse C18 columns (100 mm × 2.1 mm, d_p 1.8 μm, obtained from Agilent Technologies, Waldbronn, Germany). The binary mobile phase was 2% acetic acid in water (A) and pure methanol (B). The following mobile phase gradient program was applied: isocratic hold at 4 vol% MeOH (0–6 min), gradient 4–96 vol% MeOH (6–60 min), isocratic hold at 96 vol% MeOH (60–72 min) and flushing the initial mobile phase (72–76 min). The flow rate was set to 0.25 mL/min and the pressure at the viscosity maximum was 1065 bar. The separation was also conducted at low pressure (F_{min} = 0.05 mL/min and P_{max} = 220 bar) and with the same volumetric gradient program. The wine sample was detected by UV at 280 nm. The injection volume was 1.0 μL.

BSA tryptic digest sample: BSA tryptic digest was purchased from ProteaBio (500 pmol) and diluted with 100 μL of mobile phase A. A consisted of 0.10% TFA in 98/2 H2O:ACN (v/v) and B of 0.08% TFA in ACN. The tryptic digest was separated on two coupled 150 mm Zorbax RRHD StableBond C18 columns (150 mm × 2.1 mm, d_p 1.8 μm, obtained from Agilent Technologies, Waldbronn, Germany). The mobile phase gradient was run from 0 to 50 vol% B in 25, 50, 100 and 150 min, after which 65 vol% B was pumped for 10 min and 0 vol% B for 5 min [28]. The flow rate was set to 0.4 mL/min, corresponding to a pressure drop of 766 bar at the maximum viscosity. The column compartment oven temperature was set to 60 °C. The tryptic digest peptides were detected by UV at 216 nm. The injection volume was 20 μL.

Steroid sample: 18 steroids were purchased from Sigma–Aldrich (Bornem, Belgium): Estriol, Prednisolone, Hydrocortisone, Cortisone, Cortexolone, Hydrocortison acetate, Methylboldenone, Oestra-diol, Methyltestosterone, Stanozolol, Diethylstilbesterol, Dienestrol, Nortestosterone decanoate, Testosterone propionate, Ethynylestradiol 3-methylester (Mestranol), Algesterone, Progesterone, Testosterone phenylpropionate. The steroids were dissolved in acetonitrile at a concentration of 1000 μg/mL and diluted to 25 μg/mL (injection volume 1.0 μL). The steroids were separated on a 100 mm Zorbax RRHD Eclipse C18 column (100 mm × 2.1 mm, d_p 1.8 μm, obtained from Agilent Technologies, Waldbronn, Germany). The binary mobile phase was water and acetonitrile. The mobile phase gradient was run from 20 to 90 vol% ACN in 22 min, after which the column was flushed with 100 vol% ACN for 5 min and regenerated with 20 vol% ACN for 5 min. The flow rate was set to 0.85 mL/min, corresponding to a pressure drop of 1153 bar at the maximum viscosity. The separation was also conducted at low pressure (F_{min} = 0.10 mL/min and P_{max} = 167 bar) and with the same volumetric gradient program. The steroids were detected by UV at 230 nm.

To investigate the difference in viscous heating in constant pressure and constant flow rate mode, temperature measurements were performed using chromel–alumel thermocouples (J-type thermocouple wire) which were positioned on the column as indicated in Figs. S1–S3 of the Supplementary Material. To provide an optimum temperature measurement, the two separate wires of the junction were point-welded directly onto the column close to one another using an in-house built device. A TBX-68T Isothermal Terminal Block (National Instruments, USA) and a NI 435X (National Instruments, USA) PCI card were used to read out the voltages of the thermocouples; the software used for the temperature recording was VI Logger (LabVIEW 6i, National Instruments, Zaventem, Belgium). The local reference side temperature inside the thermal block was measured using a thermistor. The thermocouples were calibrated with both ice water and boiling water. The measurement frequency was 1 Hz.

Although the temperature measurements do not give the exact mobile phase temperature but the column wall temperature, they are suitable for comparing the effects of viscous heating in both elution modes.

3. Results and discussion

3.1. General agreement between the constant pressure and constant flow rate operation mode

Fig. 1a shows the separation of 7 anti-oxidants on a Zorbax Eclipse C18 50 mm column measured in the constant flow rate elution mode at a low pressure to minimize possible effects of pressure and viscous heating on the retention (P_{max} = 135 bar). The following peaks are identified in the chromatogram: (1) PG, (2) TBHQ, (3) TROLOX, (4) BHA, (5) OG, (6) LG and (7) AP. The flow rate was set at 0.20 mL/min and the initial pressure drop of 135 bar decreased to a minimum of 58 bars. Fig. 1b shows the same separation but operated in the constant pressure mode and by applying the same volumetric gradient program as in the cF-mode. The pressure was set to 135 bar and the initial average flow rate of 0.20 mL/min increased to a maximum of 0.46 mL/min. The total analysis time was 16.0 min in the cF-mode and 12.5 min in the cP-mode (a time reduction of 3.5 min or 21.8% because of the increased flow rate in the cP-mode). Fig. 1c shows that when the chromatogram obtained in constant pressure elution mode is converted to the volume-based time scale (using the delivered volume-time relationship given by Eq. (1)) a nearly perfect overlap between both modes exists, implying that both modes yield the same selectivity. The maximal difference in average retention between both modes is 0.04 min or 0.30%. The separation was operated in the B-term region, resulting in a slightly narrower and higher peaks in the cP-mode elution for the late eluting peaks where the flow rate increase is significant [10,11], e.g. see zoom-in of peak number 7.

A similar example is given in Fig. 2, showing the separation of a red wine sample on two Zorbax Eclipse C18 100 mm columns (see Section 2) in constant flow rate (Fig. 2a) and constant pressure (Fig. 2b) elution mode for the same volumetric gradient program. In the cF-mode, the flow rate was set to 0.05 mL/min and the initial pressure drop of 146 bar (4 vol% MeOH) increased to 220 bar (50 vol% MeOH) and than decreased to 100 bar at the end of the gradient (96 vol% MeOH). On the other hand, in the cP-mode, the pressure was set to 220 bar and the initial flow rate of 0.075 mL/min decreased to 0.050 mL/min and than increased to 0.108 mL/min. The constant pressure separation was performed in 287.7 min instead of 380.0 min as in the cF-mode (gain in time: 92.3 min, or 24.3%). The measured time gain is larger than the expected 19.1% in Table S2b of [10] due to the isocratic holds at 4% and 96% MeOH. Fig. 2c shows the overlay of the constant flow rate chromatogram (red) and the constant pressure chromatogram which is converted to the volume-based time scale (black). Again a good resemblance in selectivity can be found between both modes (see zoom-in A and B in Fig. 2c) because the same volumetric mobile phase gradient program was applied.

Since the separations shown in Figs. 1 and 2 were operated at low pressures, the absolute pressure difference between the constant pressure and constant flow rate was small and possible changes in selectivity between both modes due to the pressure effects are limited (see Section 3.3).

The time gain obtained by switching from the constant flow rate to the constant pressure operation mode does not only depend on the organic modifier type and the gradient program, but via the mobile phase viscosity also on the pressure [10,11] and the temperature. This is illustrated with the separation of Bovine Serum Albumin (BSA) tryptic digest on two Zorbax StableBond C18 150 mm columns (see Section 2). Fig. 3 shows the separation of BSA in the cF- and cP-mode (respectively red and black curves) for a gradient time of 25 min and a total analysis time of 40 min. In the cF-mode, the flow rate was set at 0.400 mL/min and the initial pressure drop of 711 bar (0 vol%

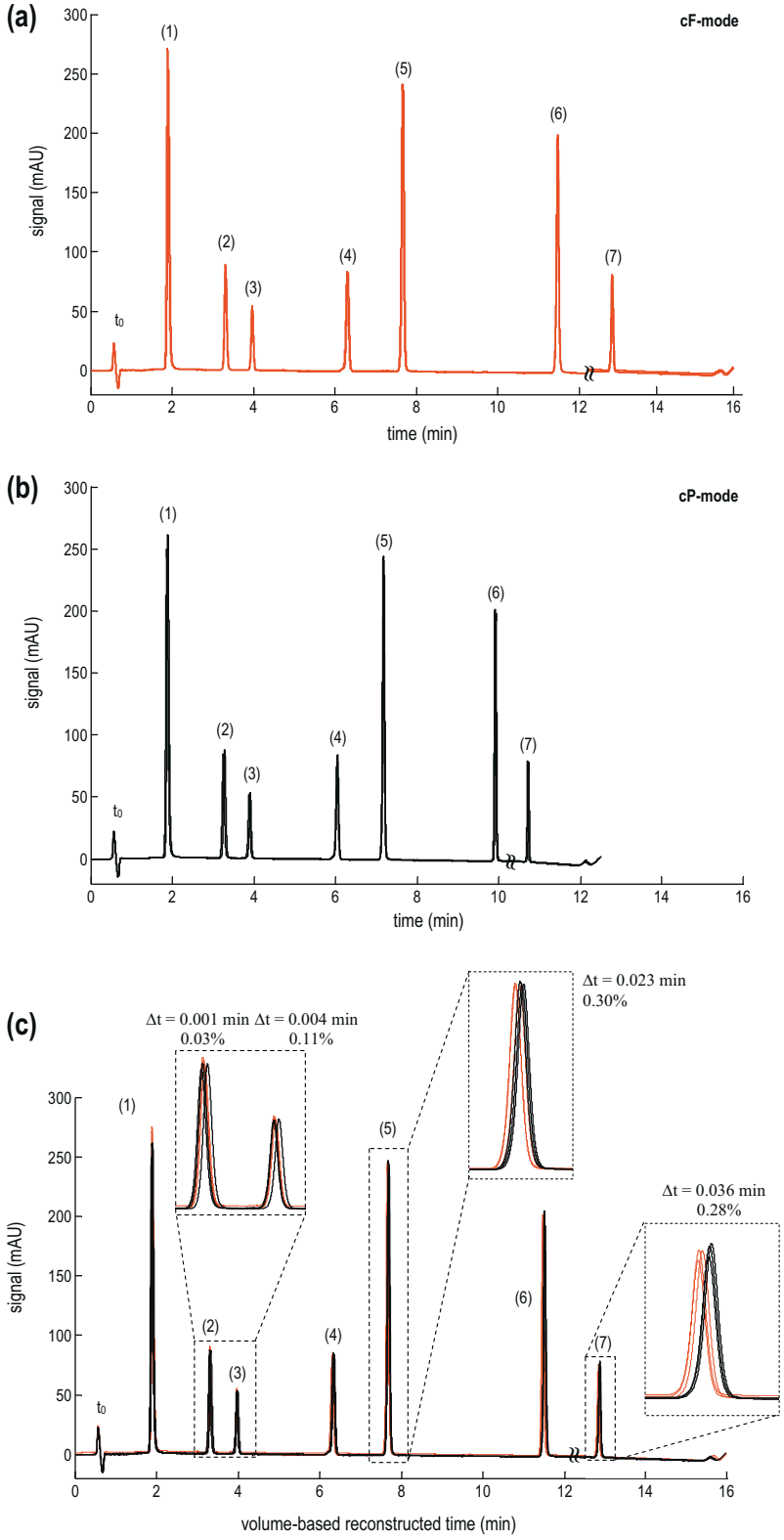

Fig. 1. Separation of 7 anti-oxidants in (a) constant flow rate (red) and (b) constant pressure (black) elution plotted in the real time scale. (c) Overlay of the constant flow rate (red) and constant pressure chromatogram converted to the volume-based reconstructed time scale (black). Mobile phase A: water with 0.02% phosphoric acid; B: 75/25 ACN:MeOH (v/v). Gradient conditions: 0–14.4 min: 30–100 vol% B and 14.4–16.0 min: 30 vol% B. F_{min} = 0.20 mL/min; P_{max} = 135 bar. Peak identities: (1) PG, (2) TBHQ, (3) TROLOX, (4) BHA, (5) OG, (6) LG and (7) AP. (For interpretation of the references to color in this figure legend, the reader is referred to the web version of the article.)

ACN) increased to 766 bar (20 vol% ACN) and then decreased to 615 bar at the end of the separation (65 vol% ACN). On the other hand, in the cP-mode, the pressure was set to 767 bar and the initial flow rate of 0.435 mL/min decreased to 0.400 mL/min and then increased to 0.495 mL/min. Fig. 3 shows very good overlap between the cF- and the reconstructed cP-signal was obtained (see the two zoom-ins in which both signals fully coincide).

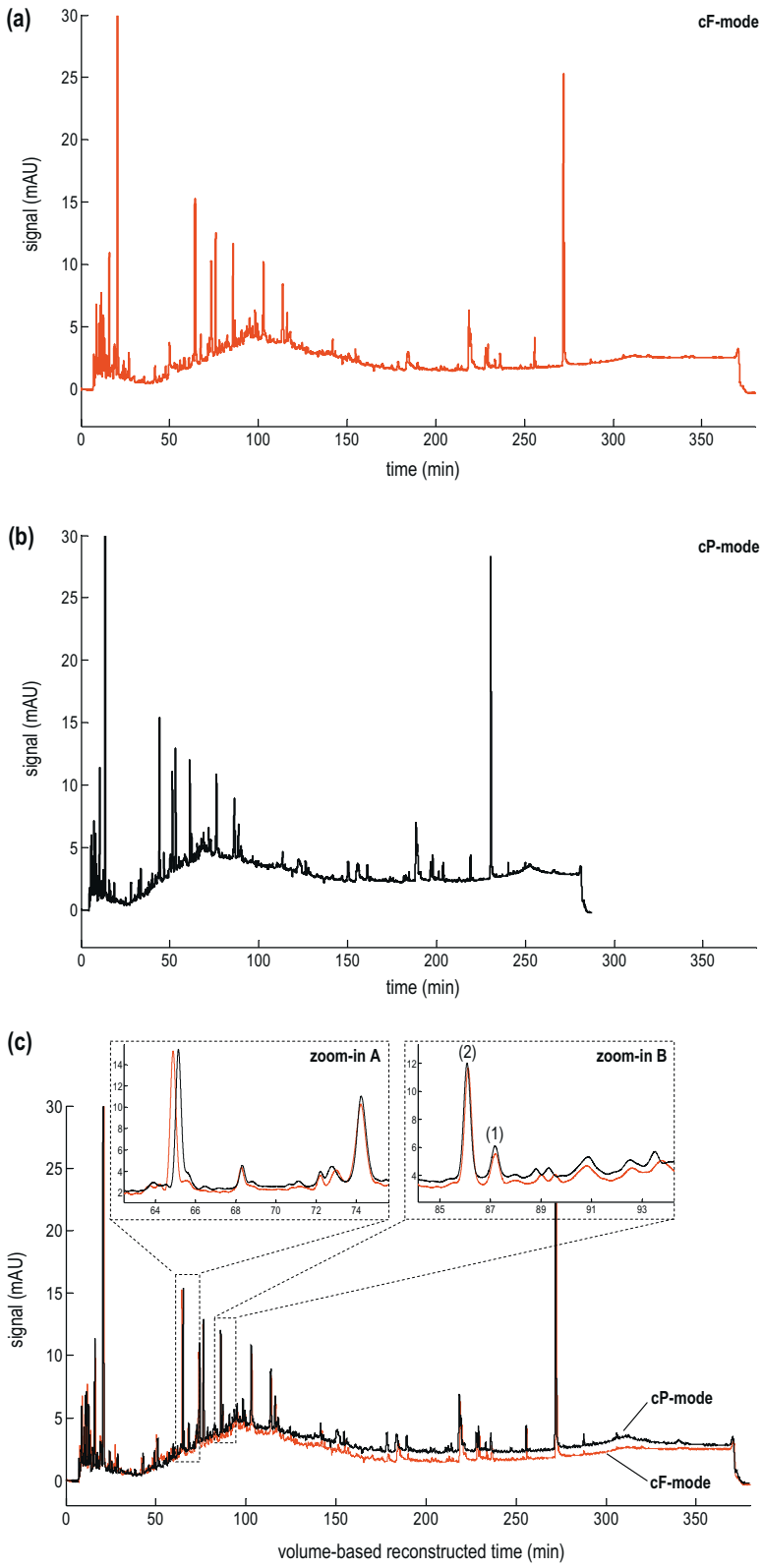

Fig. 2. Analysis of red wine in (a) constant flow rate (red) and (b) constant pressure (black) elution for an identical mobile phase gradient program. (c) Overlay of the constant flow rate (red) and constant pressure chromatogram converted to the volume-based reconstructed time scale (black). Mobile phase: MeOH:H_2O with 2% acetic acid. Gradient conditions: 0–30 min: 4 vol% MeOH; 30–300 min: 4–96 vol% MeOH; 300–360 min: 96 vol% MeOH and 360–380 min: 4 vol% MeOH. F_{min} = 0.05 mL/min; P_{max} = 220 bar. (For interpretation of the references to color in this figure legend, the reader is referred to the web version of the article.)

Table 1 shows the gain in total analysis time for the different gradient times (t_G = 25, 50, 100 and 150 min). As can be noted, the gain obtained from switching from the cF- to the cP-mode is rather small. Whereas at a temperature of 30 °C, a gain of around 8–9% can be expected for a linear gradient from 0 to 65% ACN in H_2O [10], however the measured gain during the linear part of the gradient program is only 2.4–3.1% depending on the gradient steepness. This reduced gain is caused by the operation temperature which is set

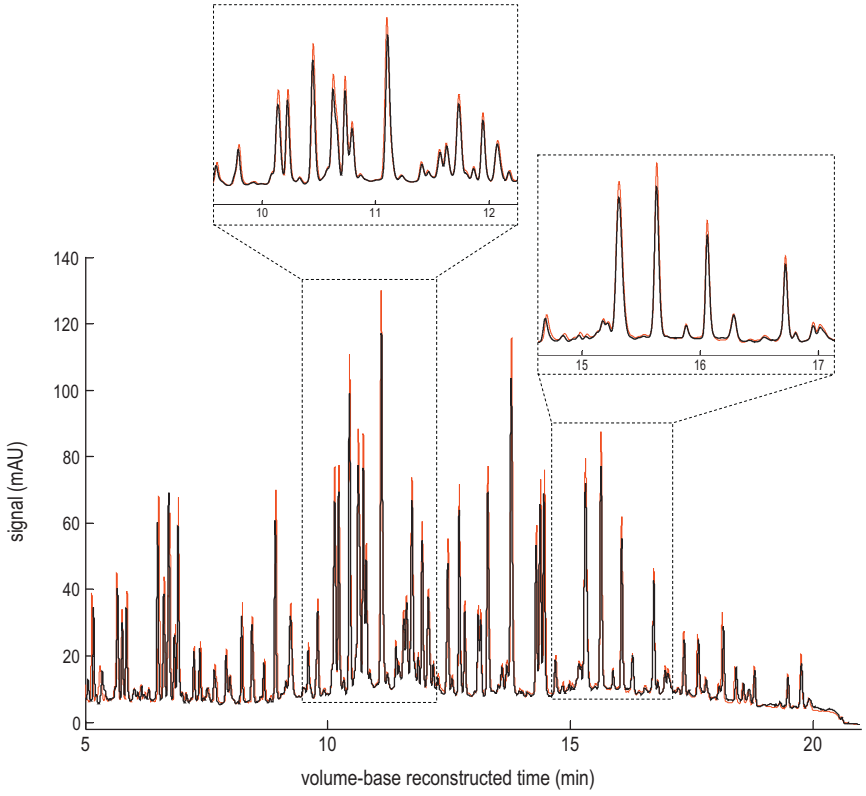

Fig. 3. Separation of BSA tryptic digest in constant flow rate (red) and constant pressure (black) elution, plotted in the volume-based reconstructed time scale. Mobile phase A: 0.10% TFA in 98/2 H_2O:ACN (v/v); B: 0.08% TFA in ACN. Gradient conditions: 0–25 min: 0–50 vol% B; 25–35 min: 65 vol% B and 35–40 min: 0 vol% B. (For interpretation of the references to color in this figure legend, the reader is referred to the web version of the article.)

to 60 °C, at which the viscosity difference between ACN and H_2O is smaller compared to the temperature of 30 °C [29]. The viscosity of H_2O largely decreases with increasing temperature whereas that of ACN only moderately decreases and hence the difference in viscosity decreases with increasing temperature, leading to a smaller increase in flow rate and a smaller time gain (this is similar to the effect of pressure, discussed in [10,11]). Table 1 also shows a small improvement in peak capacity, calculated based on the first and last peak of the chromatogram and the peak width at half height, and especially for the case of very long gradient times. The small improvement in peak capacity when switching from cF- to cP-mode is due to the fact that the separation was run in the B-term controlled regime and that the (small) increase in flow rate enhances the separation resolution. This is more pronounced for the very long gradient times, as was discussed in [10,11].

Although it can be concluded for this sample that the reduction in analysis time and improvement in separation performance when switching from the cF- to the cP-mode are very small due to the higher operation temperature at which the viscosity difference between the aqueous and organic mobile phase becomes smaller, it again provides a further example of the cP-operation mode leading to the same selectivity compared to the cF-mode.

Table 1
Total analysis time (t_A) and peak capacity (n_p) of the BSA tryptic digest separation in constant pressure and constant flow rate mode for different gradient times (t_G).

t_G (min)	Constant flow rate		Constant pressure	
	t_A (min)	n_p (/)	t_A (min)	n_p (/)
25	40	225	37.3	229
50	65	327	61.3	322
100	115	443	109.6	452
150	165	526	160.3	536

3.2. Quantitative agreement between the constant pressure and constant flow rate operation mode

The quantitative aspects concerning peak area and retention times when switching from the constant flow rate to the constant pressure elution mode were investigated with the separation of the anti-oxidants. Fig. 4 shows 10 overlaid separations of the 7 anti-oxidants on a Zorbax Eclipse C18 50 mm column measured subsequently in both constant flow rate (red) and constant pressure (black) gradient elution mode at a high pressure (P_{max} = 1140 bar); the chromatograms are plotted versus volume-based reconstructed time. In the cF-mode, the flow rate was set at 1.60 mL/min and the initial pressure drop of 1140 bar decreased to a minimum of 536 bars. On the other hand, in cP-mode the pressure was set to 1140 bar and the initial average flow rate of 1.60 mL/min increased to a maximum of 3.32 mL/min. The total analysis time was 2.00 min in the cF-mode and 1.58 min in the cP-mode (analysis time reduction of 0.42 min or 20.5%). The time gain at high pressure is smaller than the time gain at low pressures (21.8% for the separation at P_{max} = 135 bar) because of the influence of the pressure on the mobile phase viscosity profile [10,11]. The separation was operated in the C-term region, resulting in a slightly broader peak in the cP-mode elution (see the zoom-in of peak number 7).

Table 2 gives the average values and standard deviations of the volume-based retention times and peak areas obtained from the 10 subsequent injections shown in Fig. 4. This has been repeated three times (intraday) and the results are presented in Tables 2a–c.

The differences between the recalculated retention times (or equivalently retention volumes) in both modes are again very small (see also Fig. 4): the retention in the cP-mode is slightly higher than in the cF-mode especially for the late eluting peaks 5–7, although the absolute difference is smaller than 0.010 min resulting in a relative difference below 1% for all 7 peaks and all 3 data series (see

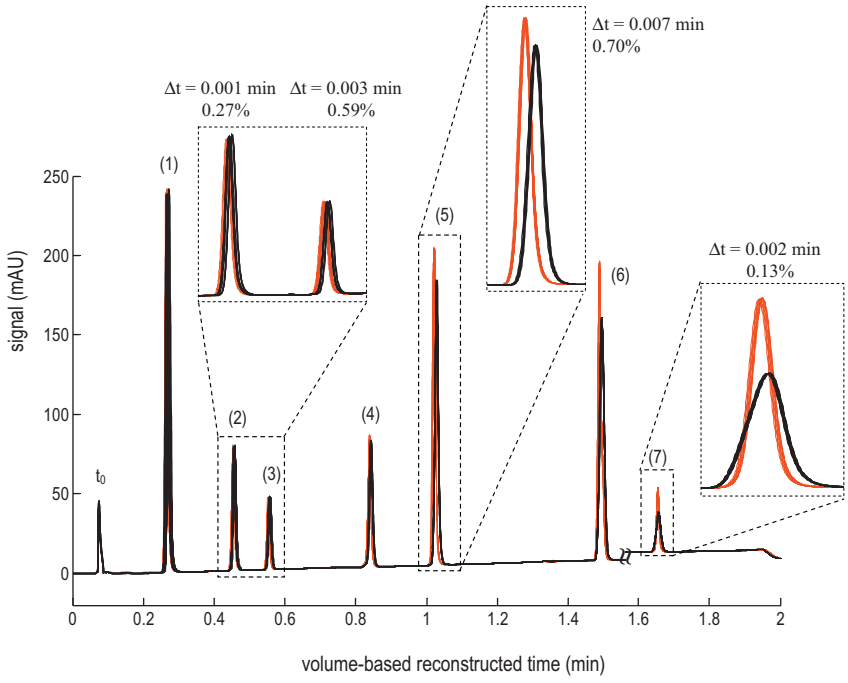

Fig. 4. Separation of 7 anti-oxidants at high pressure (F_{min} = 1.60 mL/min; P_{max} = 1140 bar) in constant flow rate (red) and constant pressure elution mode (black), plotted in the volume-based reconstructed time scale. The identical volumetric mobile phase gradient program was applied as in Fig. 1: 0–1.8 min: 30–100 vol% B and 1.8–2.0 min: 30 vol% B. Peak identities: (1) PG, (2) TBHQ, (3) TROLOX, (4) BHA, (5) OG, (6) LG and (7) AP. (For interpretation of the references to color in this figure legend, the reader is referred to the web version of the article.)

Table 2a
Mean value and standard deviation of retention time and peak area of the seven anti-oxidant compounds obtained from 10 subsequent injections in constant flow rate and constant pressure elution mode. Data series 1.

Peak number	Area *cF* (mAU s)	Area *cP* (mAU s)	Area difference (%)	Retention times *cF* (min)	Retention times *cP* (min)	Retention time difference (min)	Retention time difference (%)
1	136.26 ± 0.93	137.21 ± 0.49	0.70	0.2691 ± 0.0012	0.2688 ± 0.0028	−0.0003	0.11
2	45.08 ± 0.33	45.88 ± 0.33	1.79	0.4577 ± 0.0007	0.4589 ± 0.0016	0.0012	0.27
3	26.23 ± 0.18	26.58 ± 0.08	1.30	0.5556 ± 0.0005	0.5588 ± 0.0011	0.0032	0.59
4	51.93 ± 0.38	52.74 ± 0.13	1.56	0.8421 ± 0.0004	0.8459 ± 0.0004	0.0038	0.45
5	123.69 ± 0.38	125.22 ± 0.39	1.24	1.0241 ± 0.0004	1.0313 ± 0.0003	0.0072	0.70
6	134.82 ± 0.93	136.90 ± 0.36	1.55	1.4923 ± 0.0006	1.4990 ± 0.0002	0.0067	0.45
7	25.46 ± 0.21	25.70 ± 0.11	0.97	1.6589 ± 0.0005	1.6611 ± 0.0003	0.0022	0.13

Table 2b
Similar data as in Table 2a; data series 2.

Peak number	Area *cF* (mAU s)	Area *cP* (mAU s)	Area difference (%)	Retention times *cF* (min)	Retention times *cP* (min)	Retention time difference (min)	Retention time difference (%)
1	137.21 ± 0.34	137.66 ± 0.65	0.33	0.2690 ± 0.0011	0.2682 ± 0.0004	−0.0008	0.31
2	45.57 ± 0.20	46.10 ± 0.43	1.16	0.4565 ± 0.0008	0.4574 ± 0.0023	0.0009	0.18
3	26.46 ± 0.09	26.65 ± 0.06	0.72	0.5549 ± 0.0006	0.5575 ± 0.0018	0.0026	0.47
4	52.33 ± 0.14	52.92 ± 0.10	1.13	0.8408 ± 0.0005	0.8441 ± 0.0009	0.0033	0.39
5	124.06 ± 0.24	125.28 ± 0.30	0.98	1.0230 ± 0.0005	1.0295 ± 0.0008	0.0065	0.64
6	135.72 ± 0.30	137.08 ± 0.40	1.00	1.4904 ± 0.0005	1.4970 ± 0.0007	0.0066	0.45
7	25.28 ± 0.08	25.32 ± 0.07	0.16	1.6568 ± 0.0005	1.6594 ± 0.0005	0.0026	0.16

Table 2c
Similar data as in Table 2a; data series 3.

Peak number	Area *cF* (mAU s)	Area *cP* (mAU s)	Area difference (%)	Retention times *cF* (min)	Retention times *cP* (min)	Retention time difference (min)	Retention time difference (%)
1	137.18 ± 0.47	137.41 ± 0.63	0.17	0.2673 ± 0.0018	0.2690 ± 0.0035	0.0017	0.98
2	45.58 ± 0.27	45.95 ± 0.33	0.82	0.4547 ± 0.0010	0.4574 ± 0.0020	0.0027	0.60
3	26.44 ± 0.07	26.62 ± 0.14	0.68	0.5534 ± 0.0008	0.5576 ± 0.0014	0.0042	0.76
4	52.38 ± 0.07	52.99 ± 0.17	0.86	0.8392 ± 0.0006	0.8434 ± 0.0006	0.0042	0.50
5	123.95 ± 0.17	125.14 ± 0.32	0.96	1.0217 ± 0.0005	1.0288 ± 0.0004	0.0071	0.70
6	135.33 ± 0.44	136.54 ± 0.37	0.89	1.4888 ± 0.0005	1.4956 ± 0.0004	0.0068	0.46
7	24.74 ± 0.11	24.89 ± 0.11	0.61	1.6550 ± 0.0005	1.6575 ± 0.0004	0.0025	0.15

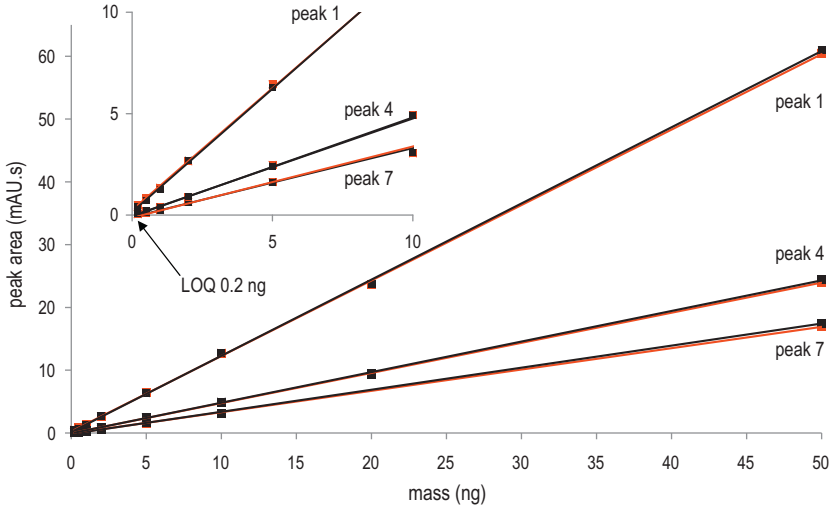

Fig. 5. Calibration curves for Propyl Gallate (peak 1), BHA (peak 4) and Ascorbil Palmitate (peak 7) in constant flow rate (red) and constant pressure (black) elution mode. The peak areas in constant pressure mode are obtained in the volume-based reconstructed time scale. (For interpretation of the references to color in this figure legend, the reader is referred to the web version of the article.)

Tables 2a–c). However, when comparing these differences in retention times to the standard deviations on the retention times in the cF-mode, it can be noted that the difference is larger than 3 times the standard deviation, which represents the 99.7% confidence interval (this can also be seen on Fig. 4: the difference in retention between both modes is larger than the variation in retention of the 10 subsequent injections in each mode). This indicates that the small difference in selectivity between the two modes is not purely random but due to the higher pressure and higher flow rate in the cP-mode compared to the cF-mode, causing physicochemical effects which will affect the selectivity. These will be further discussed in Section 3.3.

The average peak areas and the standard deviations, shown in Tables 2a–c, are also obtained from 10 subsequent injections in the cP- and cF-mode and the peak area in the cP-mode is calculated from the volume-based reconstructed signal. The difference in peak areas between both modes has an acceptable value around 1%, although that the reported peak areas in the cP-mode are slightly higher than the peak areas in the cF-mode. More importantly, for all 7 components and for the 3 data series, the differences between both elution modes (in absolute or relative values) are smaller than 3 times the standard deviation of the peak area in cF-mode, corresponding to the 99.7% confidence interval (two exceptions are peak 4 and 5 from Table 2c). This experimentally proves that the same peak areas are obtained in the cP-mode when considering volumetric units or the volume-based reconstructed time scale for a signal measured with a concentration-sensitive detector.

When comparing the standard deviation of the peak area and retention time, it can be noted that they are generally the same in constant flow rate mode as in constant pressure mode (after the volume-based conversion), indicating a similar repeatability in both modes. This also holds for the intraday repeatability. When the signal is measured in the cP-mode and processed in real time units, the repeatability of the peak area (for concentration sensitive detectors) and retention time would be much poorer compared to the cF-mode due to natural or sporadic flow resistance fluctuations in the system affecting the actual flow rate in the cP-mode.

Fig. 5 shows the calibration curves of 3 peaks which elute at the beginning of the gradient (peak 1), at the middle of the gradient (peak 4) and at the end of the gradient (peak 7). In cP-mode, the flow rate at elution is respectively 1.66 mL/min, 1.86 mL/min and 2.91 mL/min. Both the peak areas obtained in cF- and cP-mode (average of 5 subsequent injections per measured concentration) are the same and both show a linear relationship over the investigated concentration region. Table 3a shows that the slopes and intercepts of the calibration curves for the 3 peaks considered in Fig. 5 are the same (within the statistical confidence interval), as well as the fitting quality to the linear model (R^2 value). Fig. 5 also shows that both elution modes have the same limit of quantification (LOQ): this is the lowest concentration point of the calibration curve measured (0.2 ng for the calibration curves shown in Fig. 5). The limit of detection (LOD) was calculated from the calibration curves and is determined as 3 times the standard deviation (SD) on the peak area at the lowest concentration (LOQ) divided by the slope of the calibration curve. Table 3b shows that also the LOD is the same in both the cF- and cP-mode. Table 3b shows a similar conclusion for the CC_α and CC_β-values (decision limit and detection capability respectively, defined by the European Council [30]). CC_α is the limit at and above which a sample can be concluded to be non-compliant with an error probability of α. CC_β is defined as the smallest content of the substance to be detected, identified and/or quantified in a sample with an error probability of β. In the given example, CC_α values were calculated as the mean values of the smallest concentration found plus 1.64 times the corresponding standard deviation SD ($CC_\alpha = C_{found} + 1.64 \times SD$). On the other hand, CC_β values were obtained as CC_α levels plus 1.64 times the corresponding standard deviation SD ($CC_\beta = CC_\alpha + 1.64 \times SD$).

3.3. Pressure effects on the retention

As was already pointed out in the two previous sections, the difference in pressure and flow rate between both modes can affect the measured selectivity when operating under ultra high pressure conditions. In these cases, it can no longer be expected that the cP- and the cF-mode produce identical selectivities and these differences in selectivity are not unexpected in case of any method migration toward higher pressure or UHPLC. In some instances this leads to an improvement in the separation quality, but in other instances this might lead to a deterioration.

First of all, the pressure itself has an impact on the selectivity: the retention increases with increasing pressure (considering no viscous heating) [15–19]. This can be noted when comparing the separation of the anti-oxidants at low pressure (P_{max} = 135 bar, Fig. 1c) and at high pressure (P_{max} = 1140 bar, Fig. 3) for the same

Table 3a
Linear calibration curve: slope, intercept and regression quality of the constant flow rate versus the constant pressure data.

Peak number	Constant flow rate			Constant pressure		
	Slope	Intercept	R^2	Slope	Intercept	R^2
1	1.2019	0.2505	0.9998	1.2135	0.1618	0.9998
4	0.4798	−0.0345	0.9998	0.4876	−0.0598	0.9998
7	0.3401	−0.0964	0.9996	0.3510	−0.1239	0.9995

Table 3b
LOD, CC_α and CC_β of the constant flow versus the constant pressure data.

Peak number	Constant flow rate			Constant pressure		
	LOD (ng)	CC_α (ng/μL)	CC_β (ng/μL)	LOD (ng)	CC_α (ng/μL)	CC_β (ng/μL)
1	0.08	0.25	0.29	0.11	0.26	0.32
4	0.07	0.30	0.40	0.06	0.23	0.26
7	0.05	0.23	0.26	0.04	0.22	0.24

volumetric gradient program. The differences in retention times between the cP- and cF-mode are smaller for the case of the low pressure separation: 0.30% compared to the 0.70% at a high pressure for peak 5 and 0.11% compared to the 0.59% for peak 3. This shows that the retention time difference is for the most part due to pure pressure effects. For the separation at a high pressure, the maximal pressure difference between the cP- and cF-mode was ΔP_{max} = 605 bar, whereas for the separation at a low pressure, the maximal pressure difference was only ΔP_{max} = 78 bar between both elution modes.

Secondly, in the cP-mode an increase in viscous heating can be expected as a direct consequence from the higher pressure and flow rate during the cP-run. The generated heat inside the column due to viscous heating is the product of the flow rate and the pressure drop over the column [20–25]. Considering the case of an adiabatic column (isolated column wall and thus no radial heat transfer), the mobile phase temperature increase is proportional to only the pressure drop and inversely proportional to the (volumetric) mobile phase heat capacity which decreases during a mobile phase gradient of water to organic modifier. When starting at the maximum pressure, the liquid and column wall temperature will decrease in the cF-mode due to the decrease in pressure drop which contributes more than the decrease in mobile phase heat capacity. However, in the cP-mode the liquid temperature increases during the gradient run because of the constant pressure drop and the decrease in heat capacity. This is experimentally validated and the measured temperature at the end of the column in the cF- and cP-mode for the separations at high pressure is shown in Figs. S1–S3 of the Supplementary Material. Since the column is not operated under perfect adiabatic conditions, the flow rate increase in the cP-mode will result in a higher heat generation and thus higher temperature increases.

Finally, some other minor deviations between the selectivity in cP- and cF-mode are observed due to other subtle physicochemical or technical effects (e.g. such as possible pressure dependent flow rate or composition deviations due to the pump). However, their

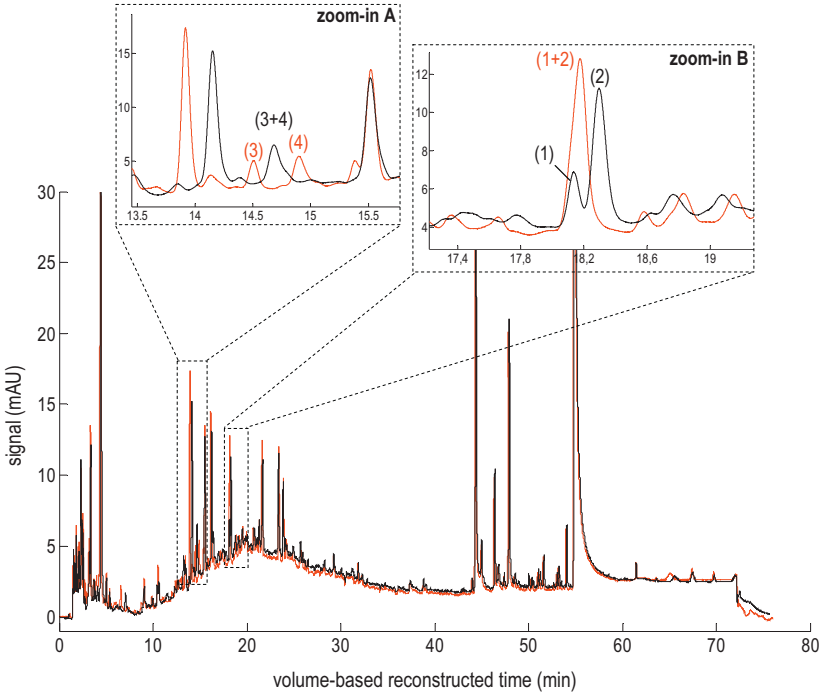

Fig. 6. Analysis of red wine at high pressure (F_{min} = 0.25 mL/min; P_{max} = 1155 bar) in constant flow rate (red) and constant pressure (black) elution, plotted in the volume-based reconstructed time scale. The identical volumetric mobile phase gradient program was applied as in Fig. 2: 0–6 min: 4 vol% MeOH; 6–60 min: 4–96 vol% MeOH; 60–72 min: 96 vol% MeOH and 72–76 min: 4 vol% MeOH. (For interpretation of the references to color in this figure legend, the reader is referred to the web version of the article.)

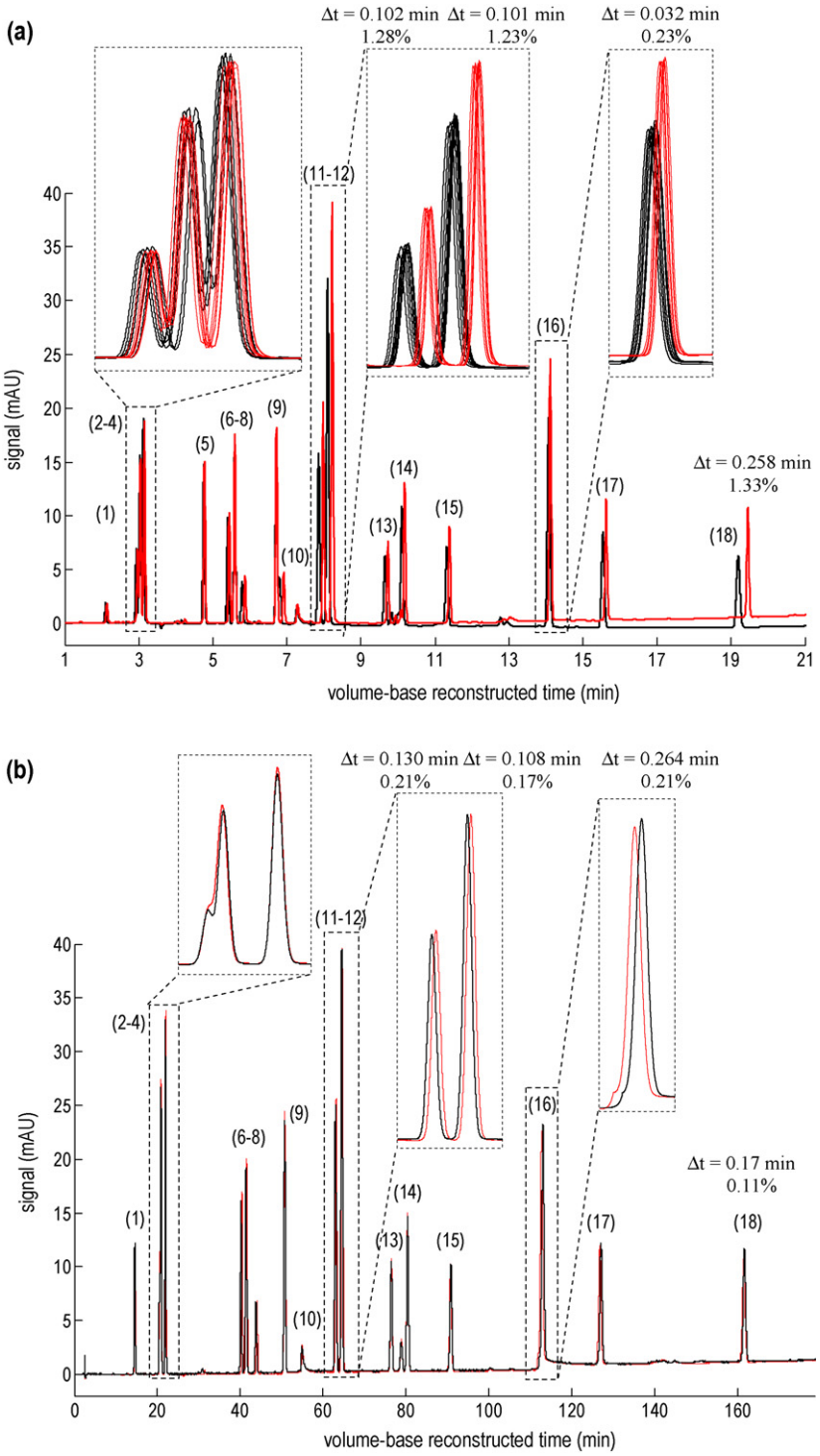

Fig. 7. Separation of 18 steroids in constant flow rate (red) and constant pressure (black) elution, plotted in the volume-based reconstructed time scale at (a) high pressure (F_{min} = 0.85 mL/min; P_{max} = 1153 bar) and (b) low pressure (F_{min} = 0.10 mL/min; P_{max} = 167 bar). Mobile phase: ACN:H_2O. Gradient conditions at high pressure: 0–22 min: 20–90 vol% ACN; 22–27 min: 100 vol% ACN and 27–32 min: 20 vol% ACN. For the separation at low pressure, the identical volumetric gradient program was applied. Peak identities: (1) Estriol, (2) Prednisolone, (3) Hydrocortisone, (4) Cortisone, (5) Cortexolone, (6) Hydrocortison acetate, (7) Methylboldenone, (8) Oestradiol, (9) Methyltestosterone, (10) Stanozolol, (11) Diethylstilbesterol, (12) Dienestrol, (13) Nortestosterone decanoate, (14) Testosterone propionate, (15) Ethynylestradiol 3-methylester, (16) Algesterone, (17) Progestrone and (18) Testosterone phenylpropionate. (For interpretation of the references to color in this figure legend, the reader is referred to the web version of the article.)

full investigation is beyond the scope of the presented work since their contribution to the differences in retention times between both modes is very moderate (<0.5%).

Another example of the selectivity changes due to pressure driven effects is given in Fig. 6 which shows the separation of a red wine on two Zorbax Eclipse C18 100 mm columns in constant pressure (black, chromatogram in volume-based reconstructed time) and constant flow rate (red) elution mode at a high pressure; the same volumetric gradient program was applied as in Fig. 2 and zoom-in A and B of Fig. 6 have the same retention window as the zoom-ins on Fig. 2c. All separations were repeated 3 times with a high degree of repeatability. In the cF-mode, the flow rate was

Table 4
Mean value and standard deviation of the retention times of the 18 steroid compounds obtained from 10 subsequent injections in constant flow rate and constant pressure elution mode.

Peak number	Retention times *cF* (min)	Retention times *cP* (min)	Retention time difference (min)	Retention time difference (%)
1	2.120 ± 0.036	2.129 ± 0.027	0.009	0.41
2	2.948 ± 0.031	2.952 ± 0.019	0.004	0.11
3	3.032 ± 0.025	3.053 ± 0.018	0.021	0.70
4	3.137 ± 0.031	3.138 ± 0.017	0.001	0.04
5	4.763 ± 0.020	4.763 ± 0.011	0.000	0.00
6	5.433 ± 0.023	5.411 ± 0.009	−0.022	0.39
7	5.591 ± 0.010	5.610 ± 0.010	0.019	0.32
8	5.851 ± 0.030	5.796 ± 0.010	−0.055	0.94
9	6.718 ± 0.010	6.732 ± 0.009	0.014	0.22
10	7.283 ± 0.012	7.286 ± 0.009	0.003	0.04
11	7.953 ± 0.039	7.851 ± 0.016	−0.102	1.28
12	8.195 ± 0.039	8.094 ± 0.015	−0.101	1.23
13	9.706 ± 0.028	9.644 ± 0.011	−0.062	0.64
14	10.160 ± 0.027	10.101 ± 0.012	−0.059	0.58
15	11.371 ± 0.028	11.312 ± 0.014	−0.059	0.51
16	14.092 ± 0.029	14.060 ± 0.013	−0.032	0.23
17	15.599 ± 0.038	15.514 ± 0.022	−0.085	0.54
18	19.412 ± 0.060	19.154 ± 0.035	−0.258	1.33

set to 0.25 mL/min and the initial pressure drop of 676 bar (4 vol% MeOH) increased to 1050 bar (50 vol% MeOH) and than decreased to 521 bar at the end of the gradient (96 vol% MeOH). On the other hand, in cP-mode, the pressure was set to 1155 bar and the initial flow rate of 0.40 mL/min decreased to 0.25 mL/min and then increased to 0.49 mL/min. The constant pressure separation was performed in 58.2 min compared to 76.0 min in the cF-mode (gain in time: 17.8 min, or 23.4%).

At first sight, the same separation (selectivity and resolution) is obtained in both elution modes. However, as can be seen from the zoom-ins of Fig. 6, pressure and viscous heating effects result in some (minor) retention shifts of the separated compounds (the temperature profile of the red wine separation is given in Fig. S2).

Zoom-in B of Fig. 6 shows that peaks 1 and 2 co-elute in the constant flow rate mode, whereas they are adequately separated in constant pressure mode due to the higher retention of peak 2 at higher pressures. This is confirmed by zoom-in B of Fig. 2c which shows the separation at a low pressure: the same retention of peak 1 and 2 is obtained in both modes because the absolute difference in pressure is small. The inverse peak order is observed at low pressures which is a result from the fact that peak 2 is much more influenced by pressure than the retention of peak 1. Zoom-in A of Fig. 6 shows again that the increased pressure and temperature will lead to slight changes in selectivity and resolution. Whereas peaks 3 and 4 are adequately separated in the constant flow rate mode, they co-elute in constant pressure mode. The effect might be explained by that the peak 3 has an increased retention at higher pressure and peak 4 has a decreased retention due to viscous heating and the associated temperature increase. When eliminating these pressure and temperature effects (Fig. 2c, zoom-in A measured at low pressures), the selectivities and resolution remain almost unchanged when switching from constant flow rate to constant pressure elution mode.

Generally the overall effect of the pressure differences and viscous heating on the total peak count is negligible for the investigated sample: the ChemStation software detected 157 ± 8 peaks in the cF-mode compared to 158 ± 6 peaks in the cP-mode, but the latter was analyzed in 58.2 min instead of 76 min, i.e. with a reduction of 17.8 min (ChemStation detection settings: slope sensitivity 0.1; peak width 0.5; area reject 0.01; height reject 0.1; shoulders 'DROP').

Selectivity changes presumably caused by viscous heating are shown in Fig. 7a, which shows the separation of the steroid mixture on a Zorbax Eclipse C18 100 mm column in constant pressure (black, chromatogram in volume-based reconstructed time) and constant flow rate (red) elution mode at ultra-high pressure. The following components are identified: (1) Estriol, (2) Prednisolone, (3) Hydrocortisone, (4) Cortisone, (5) Cortexolone, (6) Hydrocortison acetate, (7) Methylboldenone, (8) Oestradiol, (9) Methyltestosterone, (10) Stanozolol, (11) Diethylstilbesterol, (12) Dienestrol, (13) Nortestosterone decanoate, (14) Testosterone propionate, (15) Ethynylestradiol 3-methylester, (16) Algesterone, (17) Progestrone and (18) Testosterone phenylpropionate.

In the cF-mode, the flow rate was set at 0.85 mL/min. The initial pressure drop of 1153 bar decreased to 595 bar at the end of the gradient ($t = t_G$, 90% ACN) and to a minimum of 521 bar during flushing (100% ACN). On the other hand, in cP-mode, the pressure was set to 1153 bar and the initial average flow rate of 0.80 mL/min increased to 1.54 mL/min at the end of the gradient ($t = t_G$, 90% ACN) and to a maximum of 1.72 mL/min during the flushing step (100% ACN). The total analysis time of 32.00 min in the cF-mode was reduced to 26.5 min in the cP-mode. The total time gain of 5.5 min (17.2%) can be divided into the three segments of the gradient program: 20–90% ACN in 19.3 min instead of 22 min (2.7 min gain, or 12.3%), flushing at 100% ACN in 2.3 min instead of 5 min (2.7 min gain, or 54%), flushing at 20% ACN in 4.9 min instead of 5.0 min (0.1 min gain, or 2%). This shows that, as expected, the time gain in cP-operation mode is most pronounced in the gradient segments, where the eluent viscosity is lowest. For the late eluting analytes the flow rate increase is significant and slightly broader peaks are obtained in the cP-mode because the separation is operated in the C-term region.

Table 4 shows the mean values and standard deviations of the retention times for the steroid compounds obtained from 10 subsequent injections in both the cF- and cP-mode. A small but significant difference in retention can be noted between both modes (see also Fig. 7a): e.g. for peaks 11, 12, 17 and especially 18 the retention is lower in the cP-mode, whereas the retention of peak 16 almost does not change ($\Delta t_R = 0.23\%$ for peak 16 compared to $\Delta t_R = 1.33\%$ for peak 18). The decrease in retention is presumably caused by viscous heating: Fig. S3 shows the gradient temperature profiles measured on the column wall at the end of the column. The column wall temperature varies during the gradient analysis between 38.7 °C and 32.8 °C in cF-mode and between 40.0 °C and 47.8 °C in cP-mode. The late eluting compounds will experience the largest temperature difference between both modes (T_{cP}–T_{cF} is maximally 15.0 °C), resulting in a decrease in the retention of peaks 11, 12, 17 and 18 in constant pressure elution. The more severe effect of viscous heating at high pressures in the cP-mode compared to the cF-mode is not surprising since raising the pressure leads to more viscous heating unless narrow-bore columns or an intermediate

cooling system are applied [31]. The temperature variations during the steroid separation are larger compared to the anti-oxidant separation (corresponding temperature profile in Fig. S1) because of the much longer duration of the gradient program compared to the characteristic heat-up time of the column hardware (even though the thermal mass of the column is almost twice as high in this case).

A further indication of the effect of viscous heating is provided by comparing the cP- and cF-mode chromatograms of the steroid mixtures measured at a lower pressure (F_{min} = 0.1 mL/min, P_{max} = 167 bar) at which almost no viscous heating occurs. The gradient programs are adapted such that the volumetric gradient program is maintained. Fig. 7b shows the zoom-ins of peaks 11, 12, 16 and 18, for which now a nearly perfect overlap is obtained between the cF- and cP-mode separations.

Fig. 7a also shows a slight change in resolution of the critical peak pairs 2–3 and 3–4, wherein peak 3 shifts closer to peak 4 such that the resolution between peak 2 and 3 increases ($R_S = 1.49 \pm 0.04$ in cP-mode compared to 1.37 ± 0.08 in cF-mode) and the resolution of peaks 3 and 4 decreases ($R_S = 1.35 \pm 0.03$ in cP-mode compared to 1.53 ± 0.12 in cF-mode). The increase in retention of peak 3 is due to the fact that the retention of peak 3 is much more pressure dependant than peak 2 and 4. This is confirmed by the measurements at low pressure (see zoom-in in Fig. 7b) for which peak 3 almost co-elutes with peak 2 in both the cF- and cP-mode. Although the differences are very minor, peak 3 also elutes slightly earlier in the cF-mode compared to the cP-mode at low pressure, and a slightly better separation of peaks 2–3 is obtained in the cP-mode.

Table 4 also shows good repeatability in both cF- and cP-mode: the standard deviation on the retention time (after volume-based conversion of the cP-data) is the same for both modes.

4. Conclusions

The method transfer from the customary constant flow rate to the constant pressure gradient elution mode was investigated for concentration-sensitive detectors (such as UV-absorption) and for complex and real-application separations. It was found that for low pressure methods, the same selectivity is obtained in both elution modes when the identical volumetric gradient program is applied. Although, the time gain is substantial for the given examples of the anti-oxidant and wine separations (respectively 21.8% and 24.3%), it was shown that the time gain strongly depends on the experimental conditions such as pressure, temperature and specific gradient program. For high temperature separations the analysis time gain becomes smaller since the difference in viscosity between the aqueous and organic solvents decreases.

When the cP-mode chromatogram is interpreted versus the run volume, or equivalently converted to the volume-based reconstructed time scale, the peak areas measured with concentration-sensitive detectors are identical in both the cP- and cF-mode. This leads to the same calibration curves and the same LOQ and LOD for both modes. Also coinciding standard deviations on the peak area and on the retention were found, proving identical repeatability.

For separations at high pressure in the constant pressure elution mode, viscous heating and pressure effects can influence the retention of the compounds shifting the retention factors in both directions. This was illustrated for certain compounds from the wine sample for which the retention was stronger in the cP-mode compared to the cF-mode (at high pressure), as well as certain steroids which showed a decrease in retention in the cP-mode compared to the cF-mode due to viscous heating. The maximal difference between the retention in the cF-mode and in the cP-mode was 1.33% measured at high pressure (1153 bar).

Acknowledgements

The Department of Chemical Engineering of the VUB gratefully acknowledges the loan of a modified Agilent 1290 system from Agilent Waldbronn GmbH and a University Relation grant from Agilent Technologies, University Relations and External Research. M.V. and K.B. gratefully acknowledge a research grant from the Research Foundation–Flanders (FWO Vlaanderen).

Appendix A. Supplementary data

Supplementary data associated with this article can be found, in the online version, at doi:10.1016/j.chroma.2011.10.019.

References

[1] M. Gilar, U.D. Neue, J. Chromatogr. A 1169 (2007) 139.
[2] D. Cabooter, J. Billen, H. Terryn, F. Lynen, P. Sandra, G. Desmet, J. Chromatogr. A 1204 (2008) 1.
[3] J.E. MacNair, K.D. Patel, J.W. Jorgenson, Anal. Chem. 71 (1999) 700.
[4] A. Cavazzini, F. Gritti, K. Kaczmarski, N. Marchetti, G. Guiochon, Anal. Chem. 79 (2007) 5972.
[5] K. Kaczmarski, G. Guiochon, Anal. Chem. 79 (2007) 4648.
[6] F.D. Antia, C. Horvath, J. Chromatogr. 435 (1988) 1.
[7] D. Guillarme, S. Heinisch, J.L. Rocca, J. Chromatogr. A 1052 (2004) 39.
[8] S. Heinisch, G. Desmet, D. Clicq, J.L. Rocca, J. Chromatogr. A 1023 (2008) 124.
[9] S. Heinisch, J.L. Rocca, J. Chromatogr. A 1216 (2009) 642.
[10] K. Broeckhoven, M. Verstraeten, K. Choikhet, M. Dittmann, K. Witt, G. Desmet, J. Chromatogr. A 1218 (2011) 1153.
[11] M. Verstraeten, K. Broeckhoven, M. Dittmann, K. Choikhet, K. Witt, G. Desmet, J. Chromatogr. A 1218 (2011) 1170.
[12] G. Desmet, D. Clicq, D.T.T. NGuyen, D. Guillarme, S. Rudaz, J.-L. Veuthey, N. Vervoort, G. Torok, D. Cabooter, P. Gzil, Anal. Chem. 78 (2006) 2150.
[13] S. Eeltink, G. Desmet, G. Vivo-Truyols, G. Rozing, P.J. Schoenmakers, W.Th. Kok, J. Chromatogr. A 1104 (2006) 256.
[14] G. Desmet, D. Cabooter, LC–GC Europe 22 (2009) 70.
[15] N. Tanaka, T. Yoshimura, M. Araki, J. Chromatogr. 406 (1987) 247.
[16] V.L. McGuffin, C.E. Evans, J. Microcolumn Sep. 3 (1991) 513.
[17] M.C. Ringo, C.E. Evans, Anal. Chem. 69 (1997) 4964.
[18] M.M. Fallas, U.D. Neue, M.R. Hadley, D.V. McCalley, J. Chromatogr. A 1209 (2008) 195.
[19] M.M. Fallas, U.D. Neue, M.R. Hadley, D.V. McCalley, J. Chromatogr. A 1217 (2010) 276.
[20] H. Poppe, J.C. Kraak, J.F.K. Huber, H.M. van der Berg, Chromatographia 14 (1981) 515.
[21] H. Poppe, J.C. Kraak, J. Chromatogr. 282 (1983) 399.
[22] O. Dapremont, G.B. Cox, M. Martin, P. Hilaireau, H. Colin, J. Chromatogr. A 796 (1998) 81.
[23] A. de Villiers, H. Lauer, R. Szucs, S. Goodall, P. Sandra, J. Chromatogr. A 1113 (2009) 84.
[24] M.M. Fallas, M.R. Hadley, D.V. McCalley, J. Chromatogr. A 1216 (2009) 3961.
[25] F. Gritti, G. Guiochon, J. Chromatogr. A 1216 (2009) 1353.
[26] C. Perrin, L. Meyer, JAOCS 80 (2003) 115.
[27] G. Vanhoenacker, F. David, P. Sandra, Ultrafast analysis of synthetic anti-oxidants in vegetable oils using the Agilent 1290 Infinity LC system, Agilent Application Note (2009), 5990-4378EN.
[28] G. Vanhoenacker, F. David, P. Sandra, K. Sandra, B. Glatz, E. Naegele, Tryptic digest analysis using the Agilent 1290 Infinity System, Agilent Application Note (2009), 5990 4031EN.
[29] J. Billen, K. Broeckhoven, A. Liekens, K. Choikhet, G. Rozing, G. Desmet, J. Chromatogr. A 1210 (2008) 30.
[30] Commission Decision 2002/657/EC (2002) 12 August 2002 implementing council directive 96/23/EC concerning the performance of analytical methods and the interpretation of results, Off. J. Eur. Commun. L221 (2002) 8–36.
[31] K. Broeckhoven, J. Billen, M. Verstraeten, K. Choikhet, M. Dittmann, G. Rozing, J. Chromatogr. A 1217 (2010) 2022.